PHOTOCHEMICAL DEGRADATION MECHANISM OF STILBENE-1 EXAMINED BY SPECTROSCOPIC AND CHROMATOGRAPHIC METHODS

G. GAUGLITZ, R. GOES and W. SCHMID

Institut für Physikalische und Theoretische Chemie, Auf der Morgenstelle 8, D-7400 Tübingen (F.R.G.)

(Received October 18, 1985; in revised form December 16, 1985)

Summary

The prerequisite of any quantitative evaluation of a photochemical reaction is to know the mechanism. To increase the photostability of the laser dye stilbene-1 the optimal photodegradation reaction conditions must be found, and thus the mechanism was determined using a combination of chromatographic and spectroscopic techniques. Employing an optical multichannel analyser made it possible to use fluorescence spectroscopy data in the sophisticated photokinetic calculations. The mechanism and the results are discussed in detail.

1. Introduction

Stilbene-1 is a very commonly used laser dye in the blue [1]. Its laser efficiency is moderate and decreases rather rapidly because of high rates of photobleaching [2]. The solvent used is ethylene glycol, which is quite expensive and thermally unsuitable because of Schlieren effects. Photokinetic investigations proved that the first step of the sequential reaction of the photodegradation is responsible for the loss in laser activity [3].

The task is to reduce the rate of this first step by varying the pump conditions, the solvent and the chemical derivatization. For this reason quantitative reaction constants had to be obtained for comparison. Therefore it was necessary to examine the mechanism of the photodegradation to be able to set up the correct rate equations and to calculate the so-called partial photochemical quantum yields [4] as comparable parameters.

The simplest mechanism that may be assumed for the first step of the photodegradation is of the type $A \xrightarrow{h\nu} B$. But the quantum yields determined using this mechanism indicated a dependence on the wavelength of irradiation. By comparing the structures of *n*-stilbene and stilbene-1, it became obvious that their mechanisms of photoreaction are related. *n*-Stilbene follows a sequential photoreaction mechanism in which the first

0047-2670/86/$3.50

step is a reversible photoisomerization [5]. The existence of a corresponding mechanism for stilbene-1 had to be proven. Furthermore, experimental methods had to be developed to enable sufficient data points to be obtained at different wavelengths simultaneously for this rather fast first step. Fluorescence spectroscopy had to be used to observe the degradation, since to begin with the reactants and their absorptivities were unknown and therefore absorption spectroscopy would have given no quantitative information regarding the quantum yields [4].

To obtain the mechanistic information and the quantum yields, chromatographic and spectroscopic methods were developed; the fluorescence intensities were measured by a conventional fluorometer system as well as by an optical multichannel analyser arrangement to record many wavelengths simultaneously, graphical evaluations were adopted and for the first time the methods of formal integration [4, 6] were applied to measurements of fluorescence intensity, *i.e.* formal concentration–time equations were numerically integrated.

2. Apparatus

Absorption reaction spectra were recorded using a microprocessor-controlled combined irradiation and measurement device [7] containing a DMR 10 double-beam spectrometer (C. Zeiss, Oberkochen), an St75 mercury arc (Quarzlampengesellschaft Hanau) and a TM 990 microprocessor (Texas Instruments, Freising) which is part of a Labdata station [8]. The absorption spectra can be recorded, digitized and stored on tape after chosen reaction times, or the obtained data can be reduced to the absorbances at characteristic wavelengths and stored for further evaluation.

Because of the unknown absorptivities of the photoconsecutive products the photokinetic data were obtained by measuring the dependence of the fluorescence intensity on the irradiation time either by using a ZFM-4 fluorometer set-up (C. Zeiss, Oberkochen) [8] or by using the optical multichannel analyser arrangement (OMA) previously used for other time-critical experiments [9]. Figure 1 is a block diagram of the OMA. The OMA is substituted for the photomultiplier of the fluorometer and allows complete spectra to be recorded rather than measurements at a single wavelength, with a repetition rate of 1 Hz. Both set-ups are controlled by the Labdata station. It consists of a TM 990 microprocessor, 256 KByte dynamic RAM, two disk drives (each 1 MByte storage capacity), a 12-bit ADC and high resolution graphics. The PDOS operating system was constructed by Eyring (Provo, Utah) [10]; this is a multitasking and multiuser system, especially designed for process control and laboratory applications. The irradiation source (St48 mercury arc, Quarzlampengesellschaft Hanau) causes both the photodegradation and the fluorescence excitation, the latter being proportional to the concentration of the educt. The decrease in the fluorescence intensity was either recorded on the Y–t-chart drive, digitized by the

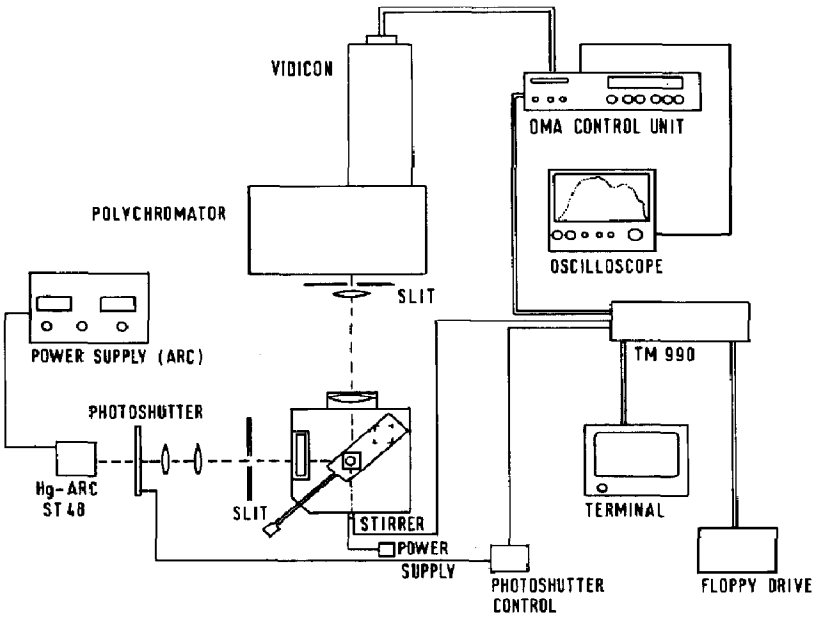

Fig. 1. Block diagram of the OMA device for the irradiation, measurement of the fluorescence intensity, data acquisition and processing.

ADC and stored on disk, or was taken as a spectrum from the control unit of the OMA and preprocessed immediately by the Labdata station. The irradiation wavelengths were selected by interference filters (UV-PIL 365, 334, 313 and 254 nm; Schott & Gen., Mainz).

The reaction chromatograms [11] were obtained by a high performance liquid chromatography apparatus combined with the Labdata station described above [12]. The apparatus applies a normal pressure cycle to the irradiated solution, which is circulated by a medium pressure pump (FMI model RP G 400; Fluid Metering Inc., U.S.A.) through a QS 110 cell (Hellma, Hanau) and an NZ 190 switch valve (Gynkotek, Munich). The microprocessor of the Labdata station controls the photoshutter for defined irradiation times and the injection of 20 μl in the high pressure cycle after chosen times. The 300 B high pressure pump, the gradient former and the SP 4 UV detector were all obtained from Gynkotek. The chromatograms were recorded on a $Y-t$ chart as well as being digitized by the ADC. They could be graphed immediately on a display or stored on disk or Winchester drive, and could be post-run evaluated. Since neither reversed-phase chromatography with pH variation nor addition of crown ether (18-crown-6) to the eluent resulted in a separation of the cis and trans isomers, ion-pair chromatography had to be used. The two peaks could then be separated by tetrabutylammonium salt (Pic A; Waters, Eschborn) buffered in a 58vol.%-MeOH–42vol.%water mixture on an ODS RP-18 hypersil column (125 mm × 4.6 mm; Bischoff, Leonberg).

3. Results and discussion

Irradiation of stilbene-1 at the wavelengths 313, 334 and 365 nm in the fluorometer apparatus yields quantum yields whose wavelength dependence, determined using the equation

$$\dot{a} = -Q'Ia(t) \tag{1}$$

is consistent with the mechanism $A^F \xrightarrow{h\nu} B$, if the concentration a of the fluorescent educt A^F is lower than 10^{-6} M and the photokinetic factor $F(E')^{-1} = (1 - 10^{-E'})/E'$ approximates unity (E' is the absorbance at the wavelength λ' of irradiation). $Q' = \epsilon'_A\phi$ where ϵ'_A is the absorptivity of the educt at the wavelength λ' and ϕ is the photochemical quantum yield of this reaction step. The irradiance is defined as $I = 2303I_0$ (I_0 (einsteins cm^{-2} s^{-1}) is the intensity of irradiation). Since the measured fluorescence intensity $I_\alpha^F(t)$ at any observation wavelength α is proportional to $a(t)$ under the assumed conditions, a graph of the logarithm of the fluorescence intensity will allow the quantum yield to be calculated using the equation

$$\ln I_\alpha^F(t) = \ln I_\alpha^F(0) - Q'It \tag{2}$$

and using the slope $m = Q'I$ to calculate ϕ as

$$\phi = -\frac{m}{I\epsilon'_A} \tag{3}$$

The results for different solvents are given in Table 1, third column. They lead to the assumption that the mechanism is wrong, because in photochemistry quantum yields normally stay the same for irradiation in the same absorption band.

To solve the mechanistic problem the absorbance reaction spectra were recorded for irradiation into different bands of absorption at two wavelengths (365 and 254 nm) as shown in Fig. 2. Long wavelength irradiation causes the band at 320 nm to be reduced in intensity. By irradiation at 254 nm the effect is reversed and the original spectrum is nearly recovered. This can be done repeatedly, but because of a degradation step resulting from the first product, the re-reaction from the photostationary state is less than about 80%. This behaviour supports the assumption of a reversible photoisomerization in the first step. Thermal reactions were found to be negligible.

The reactants could not be separated by thin-layer chromatography so further evidence was found by recording the reaction chromatogram obtained by high performance liquid chromatography [11]. The sequence of chromatograms obtained at several irradiation times are given in Fig. 3. On the bottom left the irradiation at 365 nm is represented as a sequence of chromatograms (retention time to the right, reaction time axis to the back). After chosen irradiation times, controlled by the photoshutter, 20 μl of reaction solution are injected into the high pressure cycle. Each injection results in a chromatogram; the total series comprises a

TABLE 1

Determination of the reaction constants by graphical methods

Solvent	*Wavelength* (nm)	$\phi \times 10^{-2}$	$Q \times 10^{3}$ (l mol^{-1} cm^{-1})	$\phi_1^{A} \times 10^{-2}$	$I_\alpha^{F}(s)$ (arbitrary units)
MeOH	365	1.78 ± 0.10	5.05 ± 0.51	3.70 ± 0.35	65
MeOH	334	1.61 ± 0.19	62.73 ± 12.00	3.62 ± 0.72	95
MeOH	313	0.99 ± 0.12	8.66 ± 1.03	3.59 ± 0.44	90
Ethylene glycol	365	0.67 ± 0.06	5.02 ± 0.50	1.59 ± 0.17	88
Ethylene glycol	334	0.49 ± 0.08	27.88 ± 5.90	1.72 ± 0.35	96
Ethylene glycol	313	0.26 ± 0.05	2.18 ± 0.31	1.61 ± 0.17	96
H_2O	365	4.26 ± 0.41	4.80 ± 0.50	7.39 ± 0.71	45
H_2O	334	3.42 ± 0.77	16.57 ± 4.00	7.41 ± 1.52	88
H_2O	313	2.62 ± 0.40	17.13 ± 3.10	7.27 ± 0.96	85
NP-25	365	0.58 ± 0.05	2.91 ± 0.32	1.63 ± 0.16	84
NP-8	365	0.80 ± 0.12	2.77 ± 0.31	2.97 ± 0.20	82

In the third column the photochemical quantum yields ϕ, calculated using the wrong mechanism $A^F \xrightarrow{h\nu} B$, are listed; in the other columns the so-called pseudo quantum yields $Q = \epsilon'_A\phi_1^A + \epsilon'_B\phi_2^B$, the photochemical quantum yields ϕ_1^A of the first step of the reaction and the fluorescence intensities $I_\alpha^F(s)$ of the educt A^F in relative units at the photostationary state, using the mechanism $A^F \underset{h\nu}{\overset{h\nu}{\rightleftharpoons}} B$, are listed. (NP-8 and NP-25, nonylphenylpoly(ethylene oxide), the numerals indicating the different chain length of the poly(ethylene oxide).)

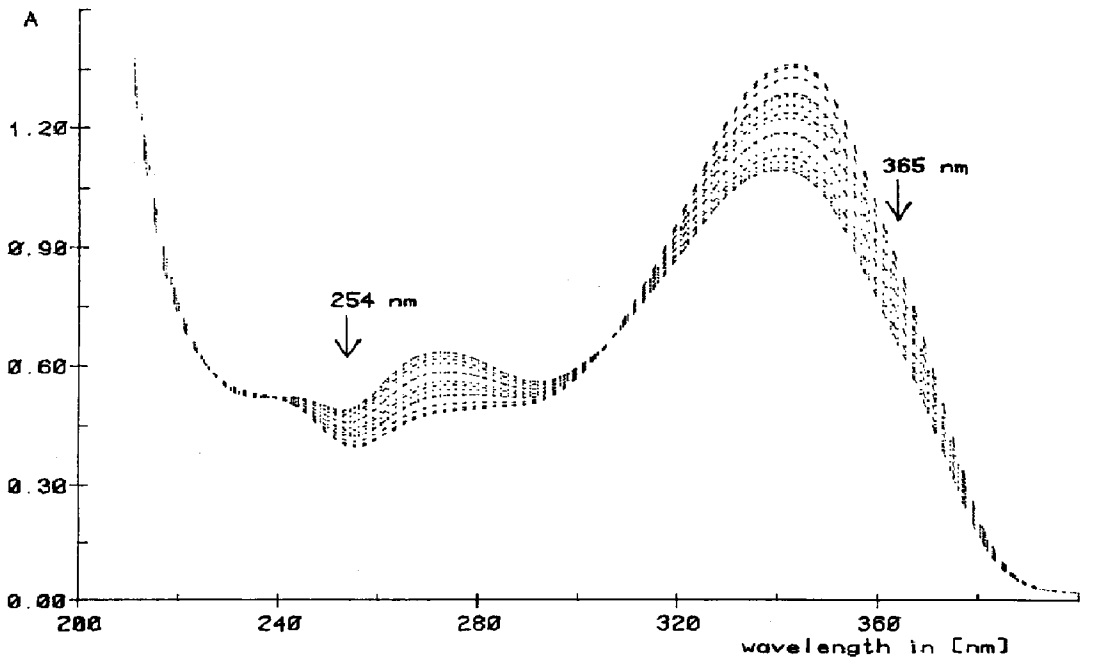

Fig. 2. Absorption reaction spectrum of the forward–backward reaction (stilbene-1 in water) by irradiation (St75 mercury arc) at λ = 365 nm and λ = 254 nm (— — —, trans–cis photoreaction (365 nm); ·····, cis–trans photoreaction (254 nm)).

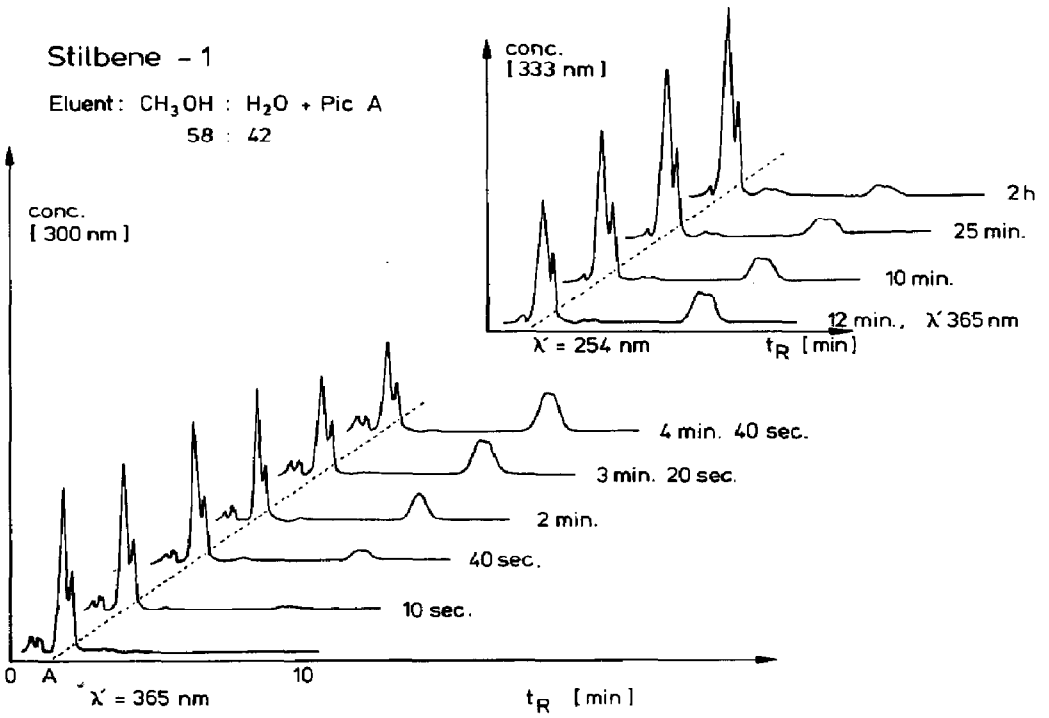

Fig. 3. Separation of stilbene-1 by ion-pair chromatography (bottom left, trans–cis photoreaction (λ = 365 nm) with formation of the cis product; top right, cis–trans photoreaction (λ = 254 nm) with removal of the cis product).

so-called reaction chromatogram. The educt peak (*trans*-stilbene-1) disappears, and at longer retention times a second peak appears until the photostationary state is reached after 4 min 40 s. Then the wavelength of irradiation is changed to 254 nm. The result is given in the graph on the top right of Fig. 3. The former second peak disappears and the original one reappears. Also, a small amount of sequential product C is formed (small peak between the educt and the first photoproduct). Considering such a reversible photoisomerization the mechanism

$$A^F \underset{h\nu}{\overset{h\nu}{\rightleftharpoons}} B$$

has to be assumed. By comparison with the stilbene photoreaction, considering the conditions of the chromatographic separation, the spectral behaviour and the reversibility of the photoreaction, the assumption of a trans–cis,cis–trans reversible photoisomerization seems reasonable. In this case instead of Q' the constant $Q = R_1 + R_2 = \epsilon'_A\phi_1{}^A + \epsilon'_B\phi_2{}^B$ has to be used. Therefore the new equation

$$I_\alpha{}^F(t) = -QII_\alpha{}^F(t) + R_2II_\alpha{}^F(0) \qquad (4)$$

is obtained. In the photostationary state ($t = s$) the equation

$$\frac{a(s)}{b(s)} = \frac{I_\alpha^F(s)}{I_\alpha^F(0) - I_\alpha^F(s)} = \frac{\epsilon'_B \phi_2^B}{\epsilon'_A \phi_1^A} = \frac{R_2}{R_1} \tag{5}$$

is valid and eqn. (4) can be written as

$$I_\alpha^F(t) = -QI\{I_\alpha^F(t) - I_\alpha^F(s)\} \tag{6}$$

$I_\alpha^F(s)$ has to be obtained by iterative fitting. For this purpose the graphical representations of the fluorescence intensity *versus* time of the sequential photodegradation are used. They show a discontinuity at the photostationary state, since the degradation rates of the first isomerization step and the later step are different. The decrease in fluorescence intensity will be caused by the consumption of educt (trans) via the preceeding equilibrium, depending on the degradation of cis to the sequential photoproduct C. By drawing tangents at the two branches of the total curve, the fluorescence intensity of the photostationary state can be approximated by extrapolation (Fig. 4). By integration of eqn. (6) a logarithmic plot will result which is analogous to that for eqn. (2). By use of this iteratively fitted value of $I_\alpha^F(s)$ the partial photochemical quantum yield of the trans–cis step can be calculated from the slope according to

$$\phi_1^A = -\frac{m}{I\epsilon'_A} \frac{I_\alpha^F(0) - I_\alpha^F(s)}{I_\alpha^F(0)} \tag{7}$$

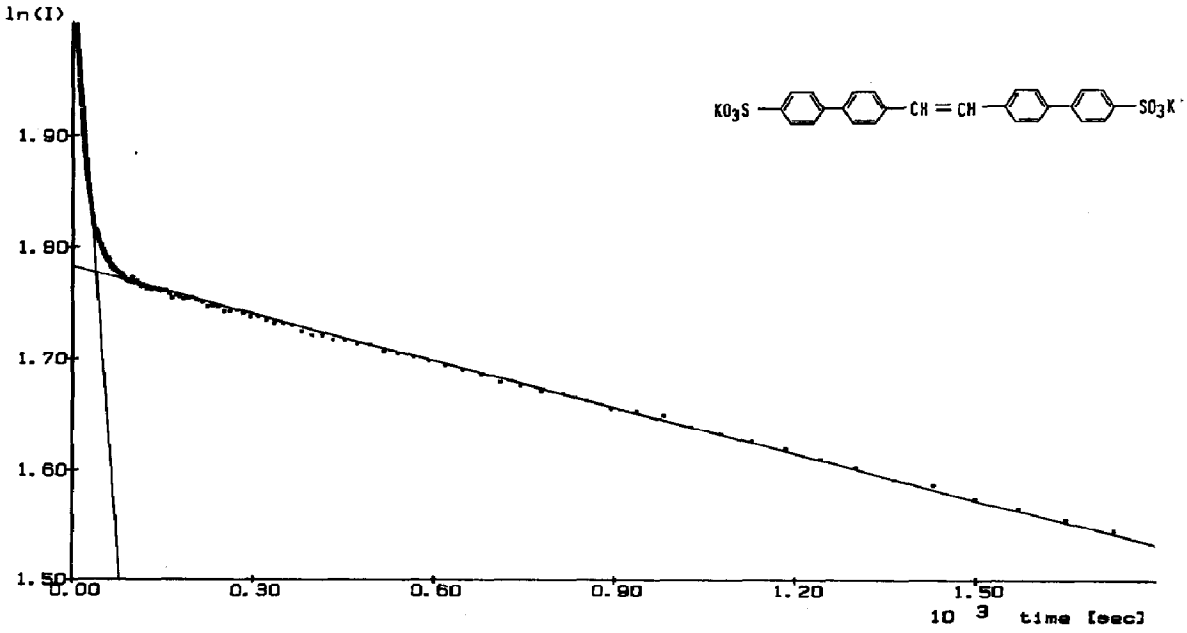

Fig. 4. ln I–t diagram for stilbene-1 in MeOH (irradiated at 365 nm, ZFM 4; detection wavelength, 410 nm): the natural logarithm of the fluorescence intensity *vs.* time, and the tangents drawn to obtain the $I_\alpha^F(s)$ values at the photostationary state.

even for unknown absorptivities of the cis isomer. This method has a great advantage in comparison with absorbance evaluations, which cannot give this information. The results for Q and $\phi_1{}^A$ are given in the fourth and fifth columns of Table 1.

A slight change in the approximated values of $I_\alpha{}^F(s)$ can cause a rather large variation in the calculated partial photochemical quantum yields. However, it is known from absorption spectroscopy that formal integration [4] has the advantage that is not necessary to know the quantity $I_\alpha{}^F(s)$; to the contrary, it is one of the results obtained in the evaluation of the equation

$$\int_0^t dI_\alpha{}^F(t) = -QI\int_0^t I_\alpha{}^F(t)\,dt + QII_\alpha{}^F(s)\int_0^t dt \tag{8}$$

By numerical integration and least-squares methods the constants QI and $QII_\alpha{}^F(s)$ can be calculated from the overdetermined set of linear independent equations for a large number of irradiation times and various observation wavelengths α. Evaluation of one experiment at many wavelengths gives the advantage of a set of independent evaluations and gives a check of whether the educt is really the only fluorescent reactant. Fluorescence measurements are more noisy than absorption experiments, but it turned out that the use of the microprocessor-controlled equipment allowed very exact data sets to be obtained even with the OMA system, which is known to have rather low photometric quality. This simultaneous fluorescence measurement at many wavelengths has the benefit of giving rather accurate quantum yields for the first step of the reversible photoisomerization without requiring knowledge of product absorptivities and without the necessity of extrapolating the fluorescence intensity at the photostationary state; therefore the method can be used even in cases for which this value cannot be obtained as easily as in the experiment discussed.

In Table 2 the pseudo quantum yield Q, the $\phi_1{}^A$ and the $I_\alpha{}^F(s)$ for the same conditions, calculated using the method of formal integration, are given. The standard deviations are even smaller than for the conventional method, both agreeing within the error limits. The photodegradation of stilbene-1 increases by nearly one order of magnitude on changing the solvent from ethylene glycol to water. This rate can be reduced in water, which is a suitable solvent because of its cheapness and its thermal properties, by use of micellar solutions, as can be seen from the data given in Tables 1 and 2.

This interesting effect was verified under laser conditions. Micellar solutions stabilize the *trans*-stilbene-1 in an excimer-laser-pumped laser dye system to the same extent as in very dilute solutions. Irradiation of the dye reservoir by a high pressure mercury arc at 254 nm reduced photodegradation, as was expected according to the mechanistic information. Therefore dual wavelength operation of the pump source could be expected to stabilize the dye stilbene-1. But the additional intense irradiation at short

TABLE 2

Determination of the reaction constants using the method of formal integration

Solvent	*Wavelength* (nm)	$Q \times 10^3$ ($l\ mol^{-1}\ cm^{-1}$)	$\phi_1^A \times 10^{-2}$	$I_\alpha^F(s)$ (arbitrary units)
MeOH	365	5.21 ± 0.21	3.75 ± 0.15	64.50
MeOH	334	65.40 ± 9.80	3.66 ± 0.52	94.10
MeOH	313	7.66 ± 0.62	3.59 ± 0.29	90.10
Ethylene glycol	365	5.46 ± 0.12	1.57 ± 0.03	86.95
Ethylene glycol	334	21.50 ± 4.60	1.61 ± 0.22	97.05
Ethylene glycol	313	1.18 ± 0.12	1.59 ± 0.09	96.95
H_2O	365	4.88 ± 0.09	7.35 ± 0.16	44.95
H_2O	334	20.30 ± 4.40	7.28 ± 1.10	87.05
H_2O	313	5.13 ± 0.42	7.34 ± 0.36	85.85
NP-25	365	2.65 ± 0.10	1.61 ± 0.06	84.95
NP-8	365	2.77 ± 0.04	2.87 ± 0.04	81.05

wavelength causes additional photodegradation pathways to appear and reduces this positive effect.

The method demonstrated of supporting mechanistic theories by chromatography and of calculating partial photochemical quantum yields with small standard deviations can be applied to laser dyes. This will open up the possibility of examining variations in the properties of the medium very accurately to obtain information on its physical characteristics. Some of these experiments will be reported in a subsequent paper [13].

Acknowledgments

We thank the Bundesministerium für Forschung und Technologie (grant 13 N 5290 2), the Deutsche Forschungsgemeinschaft and the Fond der Chemischen Industrie for personal and financial support. The donation of stilbene-1 by the Bayer AG (Dr. Raue) is gratefully acknowledged.

References

1 T. F. Johnston, Jr., R. H. Brady and W. Proffitt, *Appl. Opt., 21* (1982) 2307.
2 W. Hüffer, R. Schieder, H. Telle and R. Raue, *Opt. Commun., 28* (1979) 353.
3 B. Csacsko, E. Friz, G. Gauglitz, R. Goes and T. Klink, *Proc. IXth IUPAC Symp. on Photochemistry, Pau, July, 1982*, p. 84.
4 H. Mauser, *Formale Kinetik*, Bertelsmann Universitätsverlag, Düsseldorf, 1974, p. 128 ff.
5 H. Mauser, H. J. Niemann and R. Kretschmer, *Z. Naturforsch., Teil B, 27* (1972) 1349.
6 G. Gauglitz and T. Klink, *Z. Phys. Chem. N.F., 126* (1981) 177.
7 G. Gauglitz, T. Klink and A. Lorch, *Fresenius Z. Anal. Chem., 319* (1984) 364.

8 G. Gauglitz and R. Goes, *Comput. Enhanced Spectrosc.*, *2* (1984) 159.
9 E. Friz, G. Gauglitz, T. Klink and A. Lorch, *Comput. Enhanced Spectrosc.*, *1* (1983) 49.
10 P. R. Roper, *Microproc. Microsyst.*, *8* (1984) 458.
11 G. Gauglitz, T. Klink and W. Schmid, *J. Photochem.*, *22* (1983) 285.
12 G. Gauglitz, T. Klink and W. Schmid, *Proc. Coll. Spectrosc. Int. XXIV, Garmisch-Partenkirchen, 1985*, TUA 103, p. 198.
13 G. Gauglitz, M. Guther, J. Rieth and W. Stooss, to be published.